Scientific Reports

https://doi.org/10.1038/s41598-025-32849-3

Article in Press

The coronaviral landscape across diverse mammalian species in the Northeastern United States

Received: 15 October 2025

Accepted: 12 December 2025

Published online: 20 December 2025

Cite this article as: Ibemgbo S., Compton S., Breban M.I. *et al.* The coronaviral landscape across diverse mammalian species in the Northeastern United States. *Sci Rep* (2025). https://doi.org/10.1038/s41598-025-32849-3

Sylvester Ibemgbo, Susan Compton, Mallery I. Breban, Seth Redmond, Nathan D. Grubaugh, Megan Linske, Scott Williams, Kristof Zyskowski, Gregory Watkins-Colwell, Jane Lewis, Margot Syracuse, Guillermo Risatti, Windy D. Tanner & Caroline Zeiss

The coronaviral landscape across diverse mammalian species in the Northeastern United States

Sylvester Ibemgbo[1], Susan Compton[1], Mallery I. Breban[2], Seth Redmond[2], Nathan D. Grubaugh[2], Megan Linske[3], Scott Williams[4], Kristof Zyskowski[5], Gregory Watkins-Colwell[5], Jane Lewis[6], Margot Syracuse[7], Guillermo Risatti[7], Windy D. Tanner [8], Caroline Zeiss[1*]

1. Department of Comparative Medicine, Yale University School of Medicine, New Haven, CT 06437
2. Department of Epidemiology of Microbial Diseases, Yale School of Public Health, New Haven, CT 06437
3. Department of Entomology, The Connecticut Agricultural Experiment Station, New Haven, CT 06511
4. Department of Environmental Science and Forestry, The Connecticut Agricultural Experiment Station, New Haven, CT 06511
5. Yale Peabody Museum, New Haven, CT 06511
6. New York Gaming Commission, Big Flats, NY 14814
7. Connecticut Veterinary Medical Diagnostic Laboratory (CVMDL), Department of Pathobiology and Veterinary Science, College of Agriculture, Health and Natural Resources, University of Connecticut, Storrs, CT 06268
8. Division of Public Health, University of Utah School of Medicine, Salt Lake City, UT 84112.

*Corresponding author: caroline.zeiss@yale.edu

Keywords: animal, coronaviruses, SARS-CoV-2, surveillance, white-footed mouse

Abstract

Detection of Severe Acute Respiratory Syndrome Coronavirus-2 (SARS-CoV-2) across a broad mammalian host range has prompted concern that parallel evolution of SARS-CoV-2 in animals could reignite a surge in human infection. We conducted surveillance studies to describe the coronaviral landscape of wild and domestic animals (n=889; 27 species) in the northeastern United States. We focused on the white-footed mouse (WFM) and supplemented surveillance with laboratory infection studies to assess intra-and interspecies transmission of ancestral and Omicron variants. We detected a range of coronaviruses in fecal swabs, oral swabs or stool specimens from seven species. We did not detect SARS-CoV-2 in any animal. Infection of WFM with SARS-CoV-2 confirmed their susceptibility to ancestral and Omicron variants, however viral RNA shedding declined with the latter. Intraspecies transmission was achieved only with the ancestral strain. Neither strain could be transmitted across species. Free-living WFM experienced a 4% infection rate with a recently described *Peromyscus Betacoronavirus* with high similarity to HCoV-OC43. We failed to achieve *in vivo* infection of WFM with HCoV-OC43 indicating that WFM are unlikely to transmit this virus. Our data support a model in which evolution of SARS-CoV-2 in humans may be accompanied by its declining foothold within the animal virome.

The Severe Acute Respiratory Syndrome Coronavirus-2 (SARS-CoV-2) pandemic has been accompanied by detection of the virus across an astonishingly broad mammalian host range. [1-9] In animals, conspecific transmission has been demonstrated experimentally in white-tailed deer,[10] deer mice [11,12] and skunks,[13] as well as in free-living white-tailed deer.[5,14] Multiple examples of SARS-CoV-2 spillback into humans from white-tailed deer,[5] cat, [15] mink, [16,17] and pet hamsters [18] have prompted concern that parallel evolution of SARS-CoV-2 in animals may generate a more transmissible or pathogenic variant that could reignite a surge in human infection.[19]

SARS-CoV-2 has undergone rapid evolution, with one variant succeeding another as the virus becomes increasingly transmissible in its predominant (human) host.[20] This progression has been accompanied by persistent evidence for human to animal transmission of circulating variants, [6] as well as sustained transmission within white-tailed deer.[14] Nevertheless, rates of SARS-CoV-2 seroprevalence or infection in animal samples have declined since their peak in 2020-2022.[14,21] Whether this apparent decline in rates of animal infection or exposure [21] reflects reduced affinity of later SARS-CoV-2 variants for non-human hosts, or reduced resources for surveillance studies is unclear.

In this study, we assessed the spectrum of coronaviral infection in wild and domestic animals (n=889; representing 27 species) in the northeastern United States (centered in Connecticut) using reverse transcription polymerase chain reaction (RT-PCR) and whole genome sequencing (WGS). We focused particularly on the white-footed mouse (WFM; *Peromyscus leucopus*) due to its abundance, [22] role in zoonotic transmission risk, [23] and potential as a bridge species facilitating transmission of agents between humans and white-tailed deer.[24] We supplemented surveillance studies with *in vivo* infection and transmission experiments in WFM and hamsters to explore host susceptibility and cross-species transmission risk of ancestral and Omicron SARS-CoV-2 variants. Lastly, based on our surveillance results, we explored the capacity of WFM to become infected with and transmit human HCoV-OC43.

Results

Coronaviral surveillance: Fecal swabs, oral swabs or stool specimens from a total of 889 animals were tested, of which the majority (n=482) were WFM. Locations of source animals are shown in **Figures 1** and **2.** Results of Pan-CoV RT-PCR are given in **Table 1,** and more detailed sample and sequence data given in **Supp Tables 1** and **2.** Expected disease-associated species-adapted coronaviruses were detected in eight cats (Feline coronavirus; FCoV), one dog (Canine respiratory coronavirus; CRCoV), a ferret (Ferret coronavirus) and all eight bovines yielding pan-CoV+ amplicons (Bovine coronavirus; BCoV). A feline CoV-like product was identified in a woodchuck (% nucleotide identity 95.3%; query coverage 98%). A rodent coronavirus with similarity to Rat CoV isolate 681 (GenBank: JF792616.1) was identified in three dogs (% nucleotide identity 98.6-99.1%; query coverage 99-100%) , a white-footed mouse (% nucleotide identity 93.1%; query coverage 11%) and a red panda (% nucleotide identity 98.9%; query coverage 99%). The majority of positive WFM samples (n=15) that were sequenced were most similar (% nucleotide identity 98.3-98.9%; query coverage 92-100%) to a recently described *Peromyscus*-specific coronavirus (GenBank: OR613113.1). [25] This virus is very highly related to human HCoV-OC43, a finding noted in a prior study in WFM in Utah [26] and illustrated by high similarity of RdRp fragments (% nucleotide identity 97.15%; query coverage 100%) to HCoV-OC43 (**Supp Table 2**) in three WFM. One WFM did yield a product with very high similarity to Bovine CoV (% nucleotide identity 99.3%; query coverage 100%).

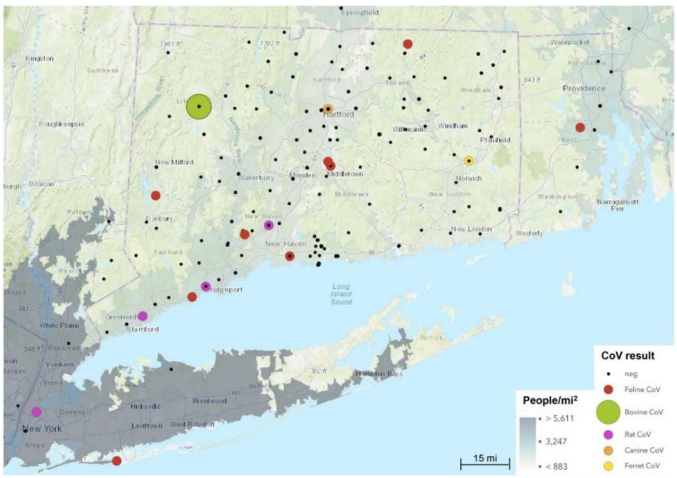

Figure 1: Locations of surveyed mammals, excluding *P. leucopus* (n=407).

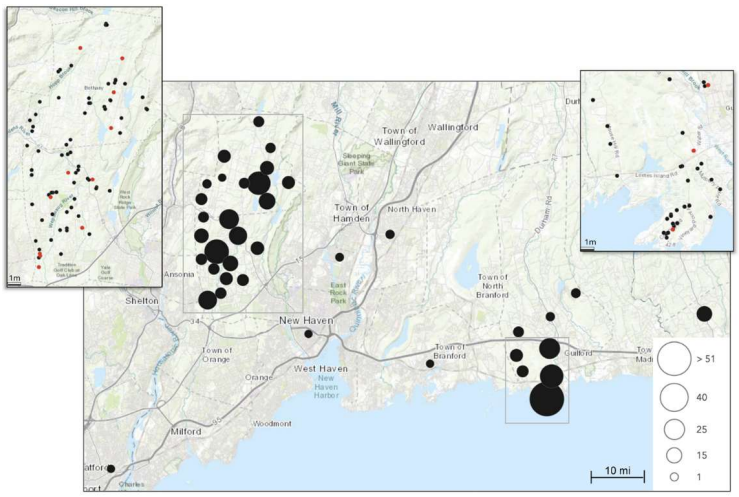

Figure 2: Locations of surveyed *P. leucopus* (n= 482).

Table 1: Pan-CoV testing results from mammalian surveillance samples, collected July 2023-June 2025 from the Northeastern United States. Sequence similarity of RdRp amplicons is expressed as percent nucleotide identity and percent query coverage.

Species	N	Pan-CoV+	Sequence similarity of RdRp amplicons
Carnivora			
Dog (*Canis familiaris*)	50	4	n=3: Rat coronavirus isolate 681 (% identity 98.6-99.1%; query coverage 99-100%) n=1: Canine respiratory coronavirus (% identity 99.3%-; query coverage 100%)
Red fox (*Vulpes vulpes*)	6	0	NA
Cat (*Felis catus*)	42	8	n=8: Feline coronavirus isolates (% identity 94.5-98.9%; query coverage 100%)
Bobcat (*Lynx rufus*)	3	0	NA
Ferret (*Mustela furo*)	1	1	n=1: Ferret coronavirus (% identity 97.3%; query coverage 99%)
Fisher (*Pekania pennanti*)	2	0	NA
Weasel (*Mustela spp*)	2	0	NA
Opossum (*Didelphis virginiana*)	5	0	NA
Raccoon (*Procyon lotor*)	43	0	NA
Striped skunk (*Mephitis mephitis*)	21	0	NA
Red Panda *(Ailurus fulgens*)	1	1	n=1: Rat coronavirus isolate 681 (% identity 98.9%; query coverage 99%)
Black Bear (*Ursus americanus*)	9	0	NA
Harbor seal (*Phoca vitulina*)	1	0	NA
Sea-lion *(Zalophus californianus)*	1	0	NA
Rodentia			
White footed mouse (*Peromyscus leucopus*)	482	18	n=9: Betacoronavirus 1 isolate Yale-225 (% identity 98.3-98.9%; query coverage 92-100%) n=1: Rat coronavirus isolate 681 (% identity 93.1%; query coverage 11%) n=1: Bovine coronavirus strain Quebec (% identity 99.3%; query coverage 100%) n=7: Not sequenced
Rat (*Rattus norvegicus*)	12	0	NA
Short-tailed shrew (*Blarina brevicauda*)	4	0	NA
Woodchuck (*Marmota monax*)	6	1	N=1: >FJ938060.1:14198-14743 Feline coronavirus UU2, complete genome (% identity 95.3%; query coverage 98%)
Red squirrel (*Sciurus vulgaris*)	4	0	NA
Artiodactyla			
White-tailed deer (*Odocoileus virginianus*)	62	0	NA
Bovine (*Bos taurus*)	92	8	n=8: Bovine coronavirus isolates (% identity 98.3-98.8%; query coverage 98-100%)

Goat (*Capra hircus*)	5	0	NA
Sheep (*Ovis aries*)	9	0	NA
Pig (*Sus scrofa*)	7	0	NA
Perissodactyla			
Horse (*Equus caballus*)	2	0	NA
Chiroptera			
Big Brown Bat (*Eptesicus fuscus*)	4	0	NA
Diprotodontia			
Wallaby (unknown species)	1	0	NA

Number of animals tested by species (N), results of pan-CoV testing, and known CoV match with highest percent identity on BLAST analysis. NA: Not applicable

Metagenomic sequencing and phylogenetic analysis: A phylogenetic analysis following multiple sequence alignment utilizing RdRp fragments of Pan-CoV samples and reference CoV viral sequences (**Supp Table 1**) is shown in **Figure 3**. The majority of samples clustered with *Betacoronavirus* reference sequences (subgenus: *Embecovirus*). These included all samples from WFM, dog, red panda and cattle, whereas remaining samples (ferret, cat and woodchuck) clustered with Alphacoronaviruses. We submitted 44 samples for metagenomic sequencing. Of these, 17 samples with sufficient signal after filtering remained (**Supp Data**). Manual BLAST analysis of contigs assembled *de novo* by CZID was performed. The majority of WFM samples confirmed results of Pan-CoV PCR testing with high similarity to a previously described *Betacoronavirus 1 isolate* (Yale). [25] Additionally, in three WFM samples, we identified an agent previously reported in *Peromyscus spp*: mouse *Mosavirus*, reported in canyon mice (*Peromyscus crinitus*). [27] Feline CoV was confirmed in two Pan-CoV positive feline samples. We did not detect SARS-CoV-2 in

any sample on metagenomic sequencing, nor did we achieve greater resolution in identification of rodent-similar viruses in dog and red panda.

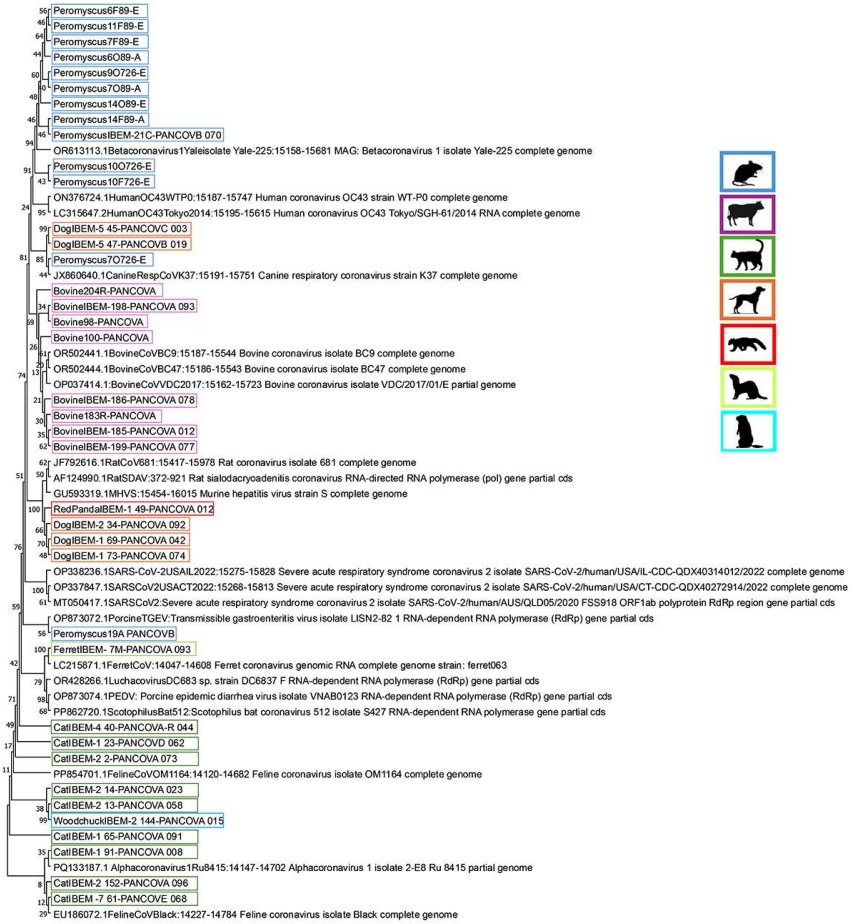

Figure 3: Phylogenetic analysis utilizing sequences derived from RdRp amplicons.

SARS-CoV-2 variant inoculation and transmission in WFM and Syrian hamsters: We assessed the capacity of the ancestral strain (SARS-CoV-2 Wuhan/IVDC-HB-01/2019) and a more recent Omicron BA5 strain [28] to infect white-footed mice and transmit between co-housed animals. We also assessed whether WFM could

transmit virus and induce disease in another susceptible species (Syrian hamster) via fomite transmission (**Supp Fig 1**). Peak oral viral RNA shedding occurred from 2-4 dpi after inoculation with the ancestral strain (**Figure 4**). This was accompanied by widespread nasal expression of viral protein by immunohistochemistry at 2 dpi (**Supp Fig 2**). Inoculation with the Omicron BA5 variant elicited a similar pattern of infection, however the extent of oral viral RNA shedding was lower and of shorter duration, with much more restricted nasal viral protein expression. With both variants, extremely rare nodular perivascular aggregates of predominantly mononuclear inflammation with occasional syncytial cells were noted at 2dpi only. Viral protein was not evident by immunohistochemistry in these lesions. The ancestral variant could be transmitted to 4 of 6 naïve white-footed mice by cohousing during the period of peak viral RNA shedding (2-4 dpi) – these animals displayed very brief shedding at 2dpi **(Figure 4**). Unlike prior studies in hamsters, [29] Omicron BA5 variant failed to transmit (**Figure 4,** defined as detection on qRT-PCR of cycle # <25) amongst WFM via direct contact. No significant changes in body weight were evident in inoculated or direct contact mice compared to mock-inoculated animals with either variant (**Supp Fig 2**), neither was evidence of extra-respiratory pathology detected. Naïve hamsters could not be infected by exposure to contaminated caging vacated by white-footed mice at the peak of their infection (**Figure 4**), nor did they develop any lung pathology at 7dpe (**Supp Fig 3**). To ensure that hamsters were susceptible to our two SARS-CoV-2 viral strains, hamsters were inoculated intranasally in a fashion similar to WFM (1X10^{e}5 PFU/animal) and euthanized at 7dpe to assess lung pathology, as previously described.[30] Consistent with our prior data using the ancestral strain, [30] this inoculum elicited abundant viral RNA shedding at 2-6dpe (**Figure 4**), accompanied by transient weight loss (**Supp Fig 3A**) and florid lung pathology. Consistent with prior reports, [31,32] inoculation with the Omicron BA5 variant elicited minimal weight loss and milder lung pathology (**Figure 4** and **Supp Fig 3B**), accompanied by lower viral RNA shedding. Taken together, these data support declining transmissibility, pathogenicity and intra-species transmissibility of a later variant (Omicron BA5) compared to the ancestral variant in two non-human animals. Further, the virus could not be transmitted across species via a low-risk route, specifically fomite exposure.

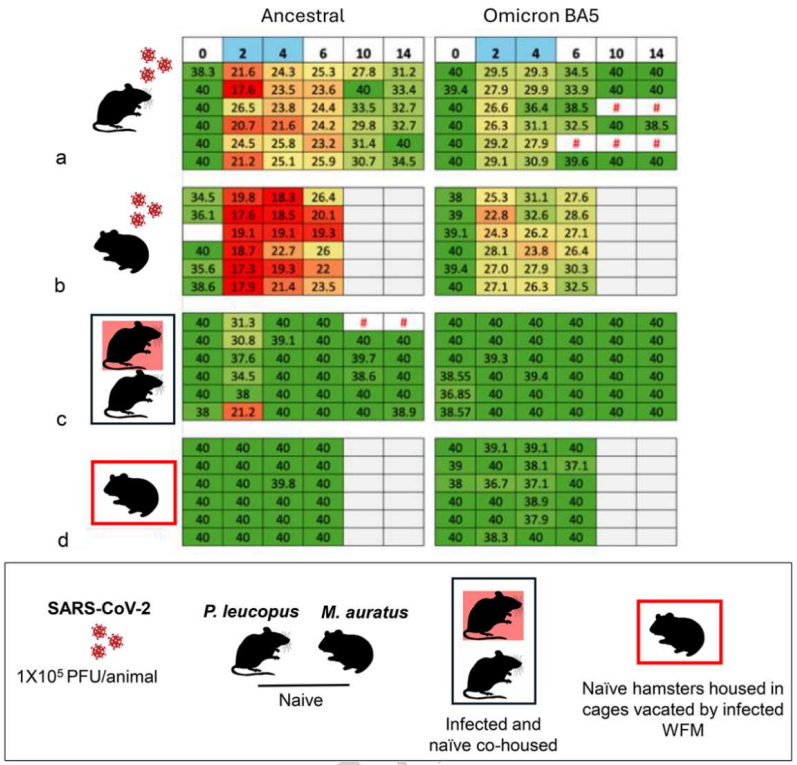

Figure 4. Viral RNA shedding (cycle number) following SARS-CoV-2 ancestral and Omicron BA5 infection in WFM and Syrian hamsters via different routes.

HCoV-OC43 infection and transmission in WFM: High similarity between the most frequently detected coronavirus in WFM and human HCoV-OC43 (**Table 1**), together with demonstrated susceptibility of a closely related rodent species (Syrian hamster) to human HCoV-OC43, [33]suggested that WFM could potentially become infected with and shed OC43 of human origin. To test this possibility, we designed inoculation and contact transmission experiments in WFM (**Supp Fig 4)**. Syrian hamsters were similarly inoculated as a positive control group for HCoV-OC43 infection.[33] Inoculated hamsters experienced

transient respiratory infection that peaked at 2 dpe and subsided by 4 dpe. In comparison to published reports, [33]extent of viral RNA shedding was both lower and more transient in our cohort. In WFM, viral shedding was lower than that seen in hamsters in inoculated mice, and absent in direct contact mice, indicating that WFM are minimally susceptible to infection by human HCoV-OC43 and do not transmit it. Viability of inoculated virus was confirmed in tissue culture (**Supp Fig 4**)

Discussion

Initial years of the COVID-19 pandemic were accompanied by detection of SARS-CoV-2 in a broad range of mammalian hosts, particularly white-tailed deer. [1-9] However, as SARS-CoV-2 becomes an established member of the human respiratory virome, [34] its position within the coronaviral landscape of other animal species is also likely to change. In this study, we searched for evidence of SARS-CoV-2 infection within the spectrum of coronaviral infection in wild and domestic animals in the northeastern United States. We focused on WFM, the most abundant peridomestic rodent in this region, [22] due to its potential for zoonotic transmission risk, [23] and as a bridge species facilitating transmission of agents between humans and white-tailed deer.[24]

Our surveillance population (n=889, across 27 species) was centered in Connecticut, but was also drawn from New York, Massachusetts and Rhode Island. As expected, we detected familiar agents such as Ferret coronavirus, [35] Bovine coronavirus, [36] Feline coronavirus [37] and Canine respiratory coronavirus [38] in domestic animals. In WFM, the majority of CoVs (79%) were most closely aligned with a *Peromyscus* coronavirus [25] within the *Betacoronavirus* 1 clade (Genus *Betacoronavirus*, Subgenus *Embecovirus*) which harbors Porcine hemagglutinating encephalomyelitis virus and Bovine coronavirus. This virus was also very highly related to human HCoV-OC43, a finding noted in a prior study in WFM in Utah. [26] To determine whether WFM could become infected with and shed HCoV-OC43, similar to a closely related Cricetulid species (Syrian hamster), [33,39] we performed experimental inoculation studies with this virus in WFM and hamsters. We confirmed that WFM inoculated with HCoV-OC43 shed minimal virus, displayed

no nasal or lung pathology and failed to transmit virus to naïve cage-mates, thus supporting the conclusion that HCoV-OC43 is unlikely to circulate between humans and WFM. In comparison to published reports, [33] extent of viral RNA shedding in inoculated hamsters was more transient in our cohort, and our hamsters failed to develop pulmonary pathology. This discrepancy may be related to differences in viral amplification and inoculation volume (100 µL at 10^5 TCID50 per animal following amplification and titering in HCT-8 cells [33]compared to direct inoculation of 30 µL at 10^5 TCID50 per animal of purchased virus in our study). Remaining CoVs identified from sequencing of Pan-CoV fragments in our surveillance study include amplicons with high similarity to a Bovine CoV isolate (from WFM), 99% similarity (over a short query length) to an uncharacterized bat CoV isolate (from a cat) and 77-99% nucleotide identity to a rodent CoV with highest similarity to Sialodacryoadenitis virus and Mouse Hepatitis Virus (in a WFM, three dogs and a red panda). We were not able to characterize these further using metagenomics.

We did not detect active SARS-CoV-2 infection in any species. A prior study in WFM and white-tailed deer conducted between 2020 and 2022 from the same geographic region [25] identified 1% and 7% seroprevalence respectively of SARS-CoV-2 neutralizing antibodies, with no evidence of active infections. Another study conducted in Virgina and Washington from May 2022-September 2023 reported 17% and 29% neutralizing antibody seroprevalence in WFM and deer mice, respectively. [6] Active infection (all variants were assigned to the XBB* Pango lineages) was detected by RT-PCR in small proportions (<5%) of *Peromyscus spp,* Virginia opossum, raccoon, Eastern cottontail rabbit and groundhogs. We did not identify SARS-CoV-2 in white-tailed deer, but recognize that fecal samples [40] may deliver a lower viral yield than sedation and direct sampling from living animals. Additionally, detection of SARS-CoV-2 in white-tailed deer varies greatly by region. [25,41-43]

Interpretation of our surveillance data was supplemented by *in vivo* infection and transmission experiments to explore within host and cross species transmissibility of ancestral and more recent (Omicron BA5) SARS-CoV-2 variants in WFM and the Syrian hamster, an established model for COVID-19. Consistent

with prior reports, [31,32] we demonstrated reduced pathogenicity of the Omicron variant compared to the ancestral strain in hamsters. This was accompanied by comparably lower viral RNA shedding in Omicron infected hamsters indicating that both pathogenicity and extent of viral shedding (and by extension, lower putative capacity to transmit virus) were reduced in this species. In WFM, a similar pattern of pathogenic attenuation in the Omicron BA5 strain compared to the ancestral strain was noted, with the added observation that WFM appeared less susceptible than hamsters to similar infectious doses of both variants. While animal-to-animal transmission of the ancestral stain was noted, viral RNA shedding in naïve cohoused animals was transient and low level. No intraspecies transmission of Omicron BA5 occurred in WFM, nor could they transmit the virus to a different species (hamsters) via fomite exposure (the most likely route of human exposure to infected white-footed mice). From these results we conclude that a later SARS-CoV-2 variant is less able to propagate within the two animal species tested than the ancestral variant. We conclude that risk of spillback transmission from WFM to humans, or bridge host transmission to white-tailed deer is extremely low.

These functional studies complement the rather complex *in vitro* data of how evolution of SARS-CoV-2 spike may affect affinity for animal Angiotensin-Converting Enzyme 2 (ACE2) receptor orthologs. [44-46] While progressive gain of affinity for mouse (*Mus musculis*) ACE2 receptor is consistently noted through Alpha, Beta, Gamma, and Omicron variants,[44,45] results for other species are quite variable. Reduced binding affinity of Omicron SARS-CoV-2 receptor binding domain to the ACE2 receptor ortholog is described in some livestock, dogs, cats and some wild animals, [44,45] whereas increased binding affinity and expanded host range is described in other studies. [45,46] The possibility that human adaptation of SARS-CoV-2 is accompanied by reduced viral fitness within other animals is supported by more recent experimental and surveillance studies. Experimental studies in cats describe reduced viral shedding and pathogenicity of the Omicron variant compared to ancestral, Gamma and Delta variants. [47] Similarly, nasal viral RNA shedding in Omicron variant-infected beagles was more transient than in Delta variant -infected animals, with lower viral RNA shedding in naïve direct contacts exposed to the Omicron inoculated group.[48]

Nevertheless, several studies describe serologic evidence of Omicron infection in wild animal species,[6,49,50] including evidence of XBB lineage circulation in wild animals in the Southeastern United States.[6]

Within-host virus expansion and diversification of human origin SARS-CoV-2 has been illustrated in large cats, hyenas [51] and white-tailed deer. [5,52] A metanalysis of 29 studies published between January 1, 2020, and May 30, 2022 indicated that the prevalence of SARS-CoV-2 in wildlife increased gradually over time. [53] A recent study in white-tailed deer [52] details continued persistence of the alpha variant in animals sampled in early 2023, almost 2 years after last human report of B.1.1.7 virus in that region. However, more recent surveillance studies describe low, [25,54,55] declining [14,21] or absent [21,41,42,56] evidence of SARS-CoV-2 in animal species. The dominant pattern revealed by surveillance data suggests a current pattern of repeated introduction of human-origin SARS-CoV-2 into animals rather than significant transmission within animal populations. [6,14,49,57-59] Despite evidence that repeated human to animal transmission of SARS-CoV-2 occurs, limited evidence of sustained animal-animal transmission can be gained from our data and recent studies [47,48,60,61] other than in white-tailed deer.[52] Our data support this trend and suggest that this apparent decline in rates of animal infection or exposure [21] may reflect reduced affinity of later SARS-CoV-2 variants for non-human hosts. Additional contributary factors include lower numbers of infected humans compared to initial surges of COVID-19 and likelyyreduced effort directed at animal surveillance studies. We note that in our study, sampling for surveillance studies occurred within subregions of a relatively restricted geographic range within the Northeast (predominantly Connecticut, with fewer samples from New York, Massachusetts and Rhode Island). Further, we utilized a PCR based assay that could miss the transient period of active SARS-CoV-2 shedding. While we failed to identify SARS-CoV-2 in this region, we cannot conclude that it is absent in animals from this region, or that similar trends prevail in other regions of the United States.

Ongoing surveillance of the coronaviral landscape in animals is a critical aspect of One Health implementation.[62] Coronaviral evolutionary flexibility and capacity for interspecies transmission is evident

in repeated examples of coronaviral disease in animals. These include evolution of new disease-causing viruses, [63,64] cross-species zoonotic infection, [65] altered tissue tropism within the same host [66] or periodic resurgences in disease severity in established hosts. [67] Long-term surveillance of wildlife and peridomestic animals provide unique opportunities to detect pathogens with zoonotic or animal health potential. We have described the baseline coronaviral landscape in the Northeast against which future surveillance findings may be compared.

Methods

Ethics Statements: All animal work was conducted under approved Yale University IACUC protocols (protocol # 2023-20523 and 2023-20491) and according to the ARRIVE guidelines.[68] We followed wild animal capture and handling protocols approved by the Wildlife Division of the Connecticut Department of Energy and Environmental Protection (permit #s 0926001b and 2125002) and the Connecticut Agricultural Experiment Station's (CAES) Institutional Animal Care and Use Committee (IACUC) (P38-22) in accordance with the American Society of Mammologist's guidelines for the use of wild animals in research.[69] For euthanasia of experimental animals, we followed the American Veterinary Medical Association (AVMA) Guidelines for the Euthanasia of Animals (2020).

Domestic and wild animal sample collection: Deceased wild and domestic animals submitted through the Connecticut Veterinary and Medical Diagnostic Laboratory (CVMDL; Storrs, CT) from CT, MA, RI and NY (**Table 1**; **Figure 1**) received oral and rectal swabs using sterile flocked swabs (Hydraflock, Puritan Medical Products, Guilford, ME). These were placed in screw top tubes with 350µl inactivating viral transport medium (PrimeStore MTM, Longhorn, Bethesda, MD). Swabs (nasal and/or rectal) were collected from swine and bovine herds in the course of routine herd surveillance conducted by the CT Department of Agriculture and submitted to the CVMDL. Tubes generated from these three sources received a unique identifier generated by the CVMDL laboratory management system. Samples were shipped to Yale with an accompanying spreadsheet including lab identifier, species, source of sample, date of collection and county

level origin of the animal. Between Nov 2023-Jan 2024, fecal samples (n=59; 1 pellet per fecal deposit) were opportunistically collected from free-living deer in Guilford, CT, placed in screw top tubes with 350µl of PrimeStore MTM, and uniquely identified by date and co-ordinates of sample collection. Samples were collected only if it had not rained the night before, and if they met criteria indicating relative freshness. [40,70] Swabs were stored at −80°C.

Wild rodent sample collection: Rodents from variably forested and residential areas in Connecticut (Guilford, Woodbridge, Bethany, Hamden, Clinton and Stratford) were trapped from June 2023 -August 2024 (**Figure 2**). Sherman live animal traps (LFAHD folding trap, H. B. Sherman Traps, Inc.) were baited with peanut butter, placed in the late afternoon and collected the following morning from cooperating homeowner properties. Twelve traps were placed at each location on approximately 30 m spacing along the lawn/forest ecotone. All traps were collected and occupied traps containing WFM were delivered to a central processing location while non-target animals were released, unless deceased (which is often the case with shrews). Each captured mouse was transferred to a plastic bag containing a cotton ball soaked in mineral oil:isoflurane 30% v/v (Piramal Critical Care, Inc.) for brief sedation. Sedated mice were sexed, weighed, measured (body, ear, and metatarsal length) and marked using a numbered metal ear tag (#1005–1, National Band and Tag Co.) to enable identification of recaptures. Oral and anal swabs (Puritan 6" Sterile Mini-tip Polyester Swab w/Ultra-Fine Polystyrene Handle 25–800 1PD 50) were collected and placed in screw-cap tubes containing 350ul Primestore Molecular Transport Medium (MTM, Longhorn, Bethesda, MD) or Dulbecco's Modified Eagle's medium (DMEM; Fisher Scientific, Waltham, MA). Mice were returned to the Sherman trap until fully recovered and released to their original collection site. Swabs were stored at −80°C. Samples from all surveilled animals were used for pan-coronaviral (Pan-CoV) RT-PCR, and in some cases, for whole genome sequencing (WGS). All captured mice were assumed to be *P. leucopus* as the known range of *P. maniculatus* is restricted to extreme northwestern Connecticut.[71]

Nucleic acid extraction and Pan-CoV RT-PCR testing

We mixed MTM-deactivated samples with 350ul of 70% ethanol, loaded this onto a column (QIAamp Mini Spin Column), and centrifuged at 6000g for 1 minute. After two consecutive washes with 500µl of AW1 and AW2 wash buffers at 6000g and 17900g, we dried the column by centrifugation at 17900g for 2 minutes. RNA was then eluted with 60µl of buffer AVE and stored at 80°C until RT-PCR testing.

We employed a semi-nested PCR with degenerate Pan Coronavirus primers targeting the RNA-dependent RNA polymerase (RdRp) gene. [72] During the first round of amplification, we used 10ul of 5x buffer, 2ul of dNTPs, 1ul each of forward and reverse primers (PanCoVOut_F 5'-CCAARTTYTAYGGHGGNTGG-3' and PanCoV_R 5'-TGTTGNGARCARAAYTCATGNGG), 2ul of enzyme and 4ul of template RNA, made up to 50ul with nuclease-free water. Thermal cycling for the first round was performed at 50 °C for 30mins for reverse transcription, 95 °C for 15mins for Polymerase activation and DNA denaturation followed by 35 cycles of 94ºC for 15secs, 53.4ºC for 30secs and 72ºC for 1min, and a final extension of 72ºC for 10mins. Second round amplification was performed with 1ul each of the first round PCR products added to the reaction mix (5ul of Roche 10x PCR reaction buffer, 1ul of dNTP mix, 0.4ul of Taq Polymerase) and 1ul each of primers (PanCoVIn_F5'GGTTGGGAYTAYCCHAARTGTGA-3' and the original reverse primer PanCoV_R) made up to 50ul with nuclease-free water. 1% Agarose was used in the gel electrophoresis, and samples yielding RdRp amplicons of the expected size (599–602 bp)[72] were purified using QIAquick Gel Extraction Kit according to the manufacturer's instructions and sent to the Keck Biotechnology Resource Laboratory at Yale University for sequencing.

Commented [CZ1]: Sylvester - please add sequence of reverse primer

Sequencing and analysis of RdRp Pan-CoV PCR fragments: Sanger sequencing of Pan-CoV positive fragments was performed using the BigDye™ Terminator v3.1 Cycle Sequencing Kit (Thermo Fisher Scientific, Cat# 4337457). Each sequencing reaction included a single-stranded DNA template, gene-specific oligonucleotide primers -PanCoV_A-PanCoV_E (5'-GGTTGGGAtTAtCCtAAgTGTGA-3', 5'-GGTTGGGAtTAcCCtAAgTGTGA-3', 5'-GGTTGGGAtTAtCCtAAaTGTGA-3', 5'-GGTTGGGAcTAtCCtAAgTGTGA-3', 5'-GGTTGGGAcTAtCCtAAaTGTG-3') standard deoxynucleotides (dNTPs), fluorescently labeled dideoxynucleotides (ddNTPs), DNA polymerase, and the

supplied reaction buffer. Cycle sequencing was carried out in a thermal cycler with the following conditions: an initial denaturation step at 95 °C for 45 seconds, followed by 40 cycles of 96 °C for 15 seconds, 50 °C for 5 seconds, and 60 °C for 2.5 minutes. Following the amplification, sequencing products were purified using the CleanSEQ magnetic bead protocol (Beckman Coulter, Cat# A29161) to remove excess dye terminators and reaction components. Purified products were subjected to capillary electrophoresis on an ABI 3730xl Genetic Analyzer (Applied Biosystems) equipped with a 96-capillary array. Sequence data were analyzed using the FinchTV version 1.4.0 and homologous sequences were sought using the National Center for Biotechnology Information (NCBI) Basic Local Alignment Search Tool (https://blast.ncbi.nlm.nih.gov/Blast.cgi). Multiple sequence alignments and phylogenetic tree were prepared utilizing RdRp fragments of our Pan-CoV samples and reference CoV viral sequences. We used the Clustal W [73] and MEGA11 [74] programs with default parameters and the neighbor-joining method with 1000 bootstrap replicates. Sequences for Pan-CoV fragments identified in animals in this study as well as reference sequences used for multiple sequence alignment are given in **Supp Table 1**. Additional details on sample origin, and s viruses identified in positive Pan-CoV samples by BLAST analysis are indicated by FASTA identifier with corresponding percent nucleotide identity and percent query coverage in **Supp Table 2**.

Metagenomic sequencing: For the majority of surveillance samples (noted in **Supp Table 2**) where we confirmed coronaviral PCR product specificity, we subsequently performed untargeted metagenomic sequencing adapted from methods previously described. [75] Extraction RNA was treated with DNase I (New England BioLabs, Ipswich, MA) and purified using a 1.8:1 bead-to-sample ratio of Mag-Bind® TotalPure NGS SPRI beads (Omega Bio-tek, Inc., Norcross, GA). First-strand cDNA was synthesized using Superscript IV VILO (Thermo Fisher Scientific, Waltham, MA), followed by second-strand synthesis using *E. coli* DNA ligase and polymerase. cDNA was purified using the above-mentioned SPRI beads at a 1.8:1 bead-to-sample ratio. DNA libraries were prepared using the Nextera XT DNA library preparation kit for Illumina (Illumina, San Diego, CA), with modifications that use smaller-than-recommended volumes for

each reaction, omitting the DNA concentration step. Individual indexed libraries were quantified using the 1x dsDNA HS assay kit on the Qubit 4 (Thermo Fisher Scientific) and pooled together at approximately 50ng per library. Pooled libraries were purified using the above-mentioned SPRI beads at a 1.7:1 bead-to-sample ratio; base pair size distribution of the pool was determined using the Agilent High Sensitivity DNA Kit on the Bioanalyzer 2100 (Agilent Technologies, Santa Clara, CA). Sequencing was performed on an Illumina NovaSeq 6000 (paired-end 150bp) at the Yale Center for Genome Analysis, targeting at least 5million reads per individual library. We performed initial bioinformatic analysis of the sequencing data using Chan Zuckerberg ID (CZID, accessed at czid.org). [76,77] We uploaded the raw sequencing reads to CZID, which performs host filtering (i.e. removed known host species reads) and quality control steps prior to de novo and reference-guided assemblies following the documented workflow (https://github.com/chanzuckerberg/czid-workflows/wiki#infectious-disease-sequencing-platform). We filtered results to select for non-phage viruses and reads with sufficient signal strength (nucleotide (NT) reads per million; NT rPM >= 100). NTrPM refers to the number of reads aligning to a taxon in NCBI's nucleotide database, per million reads sequenced (rPM). It provides an indication of relative abundance of an organism's nucleic acid and allows a standardized comparison of the relative abundance of different taxa (in our case, non-phage viruses) between samples. We then downloaded the longest three associated *de novo* contigs assembled by czid.org and manually sought similar sequences using the Basic Local Alignment Search Tool (https://blast.ncbi.nlm.nih.gov/Blast.cgi). Detailed results of metagenomics results with metrics and comparison with sequencing results of RdRp amplicons are given in the Supp Data.

SARS-CoV-2 transmission in white-footed mice and Syrian hamsters: Experimental SARS-CoV-2 infection has been reported in deer mice (*P. maniculatus*)[11,12] but not in WFM. We assessed the capacity of the ancestral strain (SARS-CoV-2 Wuhan/IVDC-HB-01/2019) and a more recent Omicron BA5 strain to infect WFM and transmit between co-housed animals. We also assessed whether WFM could transmit virus and induce disease in another susceptible species (Syrian hamster) via fomite transmission (**Supp Fig 1**). This route was used as fomite contamination of areas of human food preparation or disposal [78] was assumed to

be the most likely means by which white-footed mice could transmit the virus to other species. Experimental precedent for this route of infection has been demonstrated for Sialodacryoadenitis virus (SDAV), a respiratory Beta-CoV in rats. [79] Two days after inoculation of WFM (n=6 per infection group) with 1X10^5 PFU of SARS-CoV-2 Wuhan/IVDC-HB-01/2019 or Omicron BA5 in DMEM, each infected mouse was moved to a clean cage with a naïve sex-matched conspecific (n=6 per infection group) for 48 hours, after which inoculated and exposed mice were separated and placed in new clean cages for the remainder of the experiment. Timing of co-housing was based on results of pilot experiments. All mice were weighed and swabbed orally and anally every 2 days until their terminal euthanasia day (14 dpi). Contaminated cages vacated by inoculated WFM at the 2 day post inoculation (dpi) timepoint were used to house naïve hamsters for a period of 7 days. Hamsters were weighed and swabbed orally every 2 days. Hamsters were euthanized at 7dpi based prior observation of peak lung pathology at this time point.[30] A total of 24 WFM, evenly split by sex, were used for inoculation and transmission experiments. Six hamsters were used in each fomite exposure group (total n=12). An additional 12 mock-inoculated (DMEM) WFM (n=6) and hamsters (n=6) were used as a negative control group. All groups were evenly split by sex. All animals were 6-7 weeks of age. Three animals were euthanized due to unrelated causes (fight wounds). Prior to our transmission experiment (**Supp Fig 1)**, we performed pilot experiments in WFM (n= 15) to confirm their susceptibility to infection and to estimate peak timing of viral shedding. In these, following intranasal inoculation, WFM were swabbed and weighed every 2 days, and euthanized at 2 days (n= 4, ancestral; n=3, Omicron BA5) and 5 days (n= 4, ancestral; n=4, Omicron BA5) post-inoculation for pathologic evaluation.

HCoV-OC43 infection and transmission in white-footed mice: The most frequently detected coronavirus in WFM mice was a beta-CoV closely related to HCoV-OC43 (**Table 1**). This finding, together with demonstrated susceptibility of a closely related rodent species (Syrian hamster) to human HCoV-OC43, [33,39] suggested that WFM could potentially become infected with and shed HCoV-OC43 of human origin. To test this possibility, we designed inoculation and contact transmission experiments in WFM as illustrated in

Supp Fig 4. Syrian hamsters were similarly inoculated as a positive control group for HCoV-OC43 infection. [33]

Viruses and propagation for rodent infections: Infection and transmission experiments using SARS-CoV-2 and HCoV-OC43 were performed in WFM and Syrian hamsters. SARS-CoV-2 Wuhan/IVDC-HB-01/2019 isolate was launched from cloned cDNA [80] by RNA transcription with T7 RNA polymerase and RNA transfection into baby hamster kidney (BHK) cells engineered to express the SARS-CoV-2 N gene and mixed with Vero E6 cells. Electroporation conditions were as previously described. [81] The primary SARS-CoV-2 stock was passaged once in Vero E6-TMPRRS2 cells,[82] yielding a titer of 2.5×10^7 PFU/mL. SARS-CoV-2 Omicron BA5 isolate was obtained from a clinical patient [28] and passaged in Vero E6-TMPRRS2 cell to yield a titer of 1.8×10^6PFU/mL. Viruses were titered by plaque assay with Dulbecco's modified Eagle medium (DMEM) containing 2% fetal calf serum and 0.6% Avicel CL-611 (FMC Biopolymers), fixation with 7% formaldehyde and staining with 1% (w/v) crystal violet in 20% (v/v) ethanol. HCoV OC43 was purchased from BEI Resources (Bethesda, MD, Cat# NR-56241). Viability of HCoV OC43 was assessed using HRT-18 cells. A total of 0.7×10^6 cells were seeded into T25 flasks and incubated at 37 °C with 5% CO_2 in DMEM supplemented with 10% fetal bovine serum (FBS) until ~80% confluency was reached. The culture medium was then removed, and cells were washed with serum-free DMEM prior to inoculation. Cells were infected with 9.8×10^5 PFU of HCoV-OC43 and incubated for 1 hour at 37 °C with 5% CO_2 in serum-free medium. Following incubation, the medium was replaced with DMEM containing 2% FBS. Supernatants were collected at 24, 48, and 120 hours post-infection (hpi), and viral RNA was quantified via qRT-PCR. Uninfected HRT-18 cells grown over a similar duration constituted a negative for viral growth.

Animals, inoculation, sampling and euthanasia: WFM (6-7 weeks old) were purchased from the Peromyscus Genetic Stock Center (University of South Carolina, Columbia, SC). Similarly aged Syrian hamsters were purchased from Envigo (Indianapolis, IN, USA). All animals were evenly split by sex.

Animals were individually housed in filter top cages on corncob bedding with cotton neslets and provided ad lib access to autoclaved pellets (2018S, Envigo, Somerset, NJ, USA) and acidified water ad lib. Rooms were maintained at 72 °F on an evenly split light cycle (7 AM/7 PM). Animals were acclimated for 5–7 days prior to infection. Animals were individually identified using ear tags. For SARS-CoV-2 and OC43 experiments, viral inoculation and animal handling was performed in a Class II biosafety cabinet within a Biosafety Level (BSL) 3 or BSL 2 facility respectively. WFM were anesthetized briefly by using the open drop method (isoflurane: propylene glycol 30% v/v). Intranasal inoculation was performed with 1×10^5 plaque-forming units (PFU) per animal of SARS-CoV-2 or OC43 in Dulbecco's Modified Eagle's medium (DMEM). Health checks were performed daily. Animals were briefly anesthetized every 2 days post inoculation (dpi) via the open drop method for weighing and collection of oral and anal swabs (Hydraflock, Puritan Medical Products, Guilford, ME). At terminal time points, animals were euthanized by using 100% isoflurane via the open drop method, followed by creation of pneumothorax.

Pathology and immunohistochemistry: Lungs were intratracheally infused with 10 ml/kg (tidal volume) of 4% paraformaldehyde (PFA):025% low-molecular-weight agarose, followed by ligation of the trachea, removal of the pluck and immersion in 4% para-formaldehyde for 48 h. Remaining tissues (brain, skull, heart, tongue, esophagus, stomach, large and small intestines, liver, spleen, kidney, reproductive tract, pancreas, cervical and mesenteric lymph nodes, salivary glands) were fixed in 10% neutral-buffered formalin. Nasal pathology was performed after immersion of the head in 4% paraformaldehyde for 1 week, followed by decalcification for 24 h, coronal sectioning of nasal passages at three levels, FFPE and sectioning at 5µm. Light microscopic images were taken using a Zeiss Axioskop and with Axiocam MrC camera. Lung histopathology was assessed in hematoxylin and eosin (H&E)-stained sections. For those subjects in which statistical comparisons were required, we used a semi-quantitative scoring system adapted from published criteria [83] that included airway, vascular and parenchymal components to arrive at a total histopathology score.[30] Immunoperoxidase stains were performed at the Yale University Department of Pathology using primary antibodies directed against SARS-CoV-2 Nucleocapsid (rabbit primary antibody,

1:100, Cat # 40143-R001, SinoBiological, Houston, TX) and anti- HCoV-OC-43 (mouse primary antibody, 1:100, clone 541-8F, Sigma Aldrich, St Louis, MO). After deparaffinization and rehydration, antigen retrieval was performed using sodium citrate buffer (10mM Sodium Citrate, 0.05% Tween 20, pH 6.0) at 95-100oC for 10 minutes. Immunostaining was performed using a Dako autostainer. Label was visualized by 0.05% 3′,3′-diaminobenzidine (DAB) as a chromogen, precipitated by 0.01% hydrogen peroxide.

Quantitative RT-PCR (qRT-PCR) of SARS-CoV-2 and OC43: Oral and anal swabs (or fecal pellets if available) were submerged in 350ul MTM (Waltham, MA, USA), mixed with 350ul of 70% ethanol and loaded onto a column (QIAamp Mini Spin Column, Qiagen, Germantown, MD). The mixture was centrifuged at 6000g for 1 minute and washed with 500ul of AW1 and AW2 consecutively. The column was dried by centrifugation at 18000g for 3 minutes, and the RNA was eluted with 60ul of buffer AVE. The eluted RNA was stored at -80 ºC until required for (q)RT-PCR.

qRT-PCR for detection of SARS-CoV-2 (forward primer RdRp 5'-CGCATACAGTCTTRCAGGCT-3'; reverse primer 5'-GTGTGATGTTGAWATGACATGGTC-3'; and β-actin forward primer 5'-ATGGCCAGGTCATCACCATTG-3' and reverse primer 5'-CAGGAAGGAAGGCTGGAAAAG-3'), was done using iTaq Universal One-Step RT-qPCR in a CFX following the manufacturer's instructions. Amplification efficiency for the primer set was tested by using serial dilutions. Each 20ul reaction contained 10ul of iTaq universal SYBR Green reaction mix, 0.25ul of iScript reverse transcriptase 0.4ul each of forward and reverse primers and 6.95ul of nuclease-free water. The thermal cycling was programmed to 50ºC for 10mins for reverse transcription reaction, 95ºC for 1min followed by 40 cycles of 95ºC for 10 secs, and 60ºC for 30 secs.

qRT-PCR for detection of HCoV-OC43 (forward primer 5'-ATGTTAGGCCGATAATTGAGGACTAT-3'; reverse primer 5'-AATGTAAGATGGCCGCGTATT-3'; and β-actin forward primer 5'-ATGGCCAGGTCATCACCATTG-3' and reverse primer 5'-CAGGAAGGAAGGCTGGAAAAG-3'), was done using iTaq Universal One-Step RT-qPCR in a CFX following the manufacturer's instructions.

Amplification efficiency for the primer set was tested by using serial dilutions and source virus as a template. Each 20ul reaction contained 10ul of iTaq universal SYBR Green reaction mix, 0.25ul of iScript reverse transcriptase 0.4ul each of forward and reverse primers and 6.95ul of nuclease-free water. The thermal cycling was programmed to 50 °C for 10 mins for reverse transcription reaction, 95 °C for 1 min followed by 40 cycles of 95°C for 10 secs, and 60 °C for 30 seconds. After normalization to β-actin expression, data were expressed as relative fold change following analysis with the $2^{-\Delta\Delta Ct}$ method. [84] A non-template control lacking viral cDNA, and a positive control with 1ul of stock SARS-CoV-2 or HCoV-OC43 was included in each amplification reaction.

Funding sources: This study was supported by the United States Department of Agriculture (Project # APP-22174). Rodent capture occurred as part of integrated tick management studies funded by the Centers for Disease Control and Prevention (U01CK000665, 75D30121P12632).

Data availability: Raw sequence data (fastq files) from surveillance samples have been submitted to GenBank (submission ID: 3012446). Accession numbers are given in Supp Table 3. Sample and reference coronaviral sequences for multiple sequence alignment are given in the Supplementary Data. Metagenomics data are publically available at czid.org under the public project named "250623_CZ02_SC2_metagenomics_host_spp". To access CZ ID (Chanzuckerberg ID) public projects, users create a free CZ ID account, then navigate to the "Discovery" page. Entering the project name given above into the search box will provide all associated data including contigs. Raw metagenomics sequence data have been submitted to the NCBI Sequence Read Archive (BioProject # PRJNA1377596).

Acknowledgements: We gratefully acknowledge the excellent laboratory and histologic expertise of Gordon Terwilliger, Michael Schadt, Arthur Nugent, and Amos Brooks. We would also like to thank Heidi Stuber, Jessica Brown, Natalie Bailey, Jamie Cantoni, Carlin Eswarakumar, Claire Turner, Melissa Tian, Hailey Carter, Madison Greiger, and Matilda Kutschinski for their assistance with rodent trapping. We are

grateful to the Peromyscus Genetic Stock Center (University of South Carolina) for provision of *P. leucopus.*

Competing interests: The authors declare no competing interests.

1 Meekins, D. A., Gaudreault, N. N. & Richt, J. A. Natural and Experimental SARS-CoV-2 Infection in Domestic and Wild Animals. *Viruses* **13** (2021). https://doi.org/10.3390/v13101993

2 Chandler, J. C. *et al.* SARS-CoV-2 exposure in wild white-tailed deer (Odocoileus virginianus). *Proceedings of the National Academy of Sciences of the United States of America* **118** (2021). https://doi.org/10.1073/pnas.2114828118

3 Delahay, R. J. *et al.* Assessing the risks of SARS-CoV-2 in wildlife. *One Health Outlook* **3**, 7 (2021). https://doi.org/10.1186/s42522-021-00039-6

4 Hale, V. L. *et al.* SARS-CoV-2 infection in free-ranging white-tailed deer. *Nature* **602**, 481–486 (2022). https://doi.org/10.1038/s41586-021-04353-x

5 Pickering, B. *et al.* Divergent SARS-CoV-2 variant emerges in white-tailed deer with deer-to-human transmission. *Nat Microbiol* **7**, 2011–2024 (2022). https://doi.org/10.1038/s41564-022-01268-9

6 Goldberg, A. R. *et al.* Widespread exposure to SARS-CoV-2 in wildlife communities. *Nature communications* **15**, 6210 (2024). https://doi.org/10.1038/s41467-024-49891-w

7 Tan, C. C. S. *et al.* Transmission of SARS-CoV-2 from humans to animals and potential host adaptation. *Nature communications* **13**, 2988 (2022). https://doi.org/10.1038/s41467-022-30698-6

8 Nielsen, S. S. *et al.* SARS-CoV-2 in animals: susceptibility of animal species, risk for animal and public health, monitoring, prevention and control. *EFSA J* **21**, e07822 (2023). https://doi.org/10.2903/j.efsa.2023.7822

9 Pourbagher-Shahri, A. M., Mohammadi, G., Ghazavi, H. & Forouzanfar, F. Susceptibility of domestic and companion animals to SARS-CoV-2: a comprehensive review. *Tropical animal health and production* **55**, 60 (2023). https://doi.org/10.1007/s11250-023-03470-1

10 Martins, M. *et al.* From Deer-to-Deer: SARS-CoV-2 is efficiently transmitted and presents broad tissue tropism and replication sites in white-tailed deer. *PLoS pathogens* **18**, e1010197 (2022). https://doi.org/10.1371/journal.ppat.1010197

11 Griffin, B. D. *et al.* SARS-CoV-2 infection and transmission in the North American deer mouse. *Nature communications* **12**, 3612 (2021). https://doi.org/10.1038/s41467-021-23848-9

12 Fagre, A. *et al.* SARS-CoV-2 infection, neuropathogenesis and transmission among deer mice: Implications for spillback to New World rodents. *PLoS pathogens* **17**, e1009585 (2021). https://doi.org/10.1371/journal.ppat.1009585

13 Francisco, R. *et al.* Experimental Susceptibility of North American Raccoons (Procyon lotor) and Striped Skunks (Mephitis mephitis) to SARS-CoV-2. *Front Vet Sci* **8**, 715307 (2021). https://doi.org/10.3389/fvets.2021.715307

14 Marques, A. D. *et al.* Evolution of SARS-CoV-2 in white-tailed deer in Pennsylvania 2021-2024. *PLoS pathogens* **21**, e1012883 (2025). https://doi.org/10.1371/journal.ppat.1012883

15 Sila, T. *et al.* Suspected Cat-to-Human Transmission of SARS-CoV-2, Thailand, July-September 2021. *Emerg Infect Dis* **28**, 1485–1488 (2022). https://doi.org/10.3201/eid2807.212605

16 Hammer, A. S. *et al.* SARS-CoV-2 Transmission between Mink (Neovison vison) and Humans, Denmark. *Emerg Infect Dis* **27** (2020). https://doi.org/10.3201/eid2702.203794

17 Oude Munnink, B. B. *et al.* Transmission of SARS-CoV-2 on mink farms between humans and mink and back to humans. *Science (New York, N.Y.)* **371**, 172–177 (2021). https://doi.org/10.1126/science.abe5901

18 Yen, H. L. *et al.* Transmission of SARS-CoV-2 delta variant (AY.127) from pet hamsters to humans, leading to onward human-to-human transmission: a case study. *Lancet* **399**, 1070–1078 (2022). https://doi.org/10.1016/s0140-6736(22)00326-9

19 Bansal, N., Yendluri, V. & Wenham, R. M. The molecular biology of endometrial cancers and the implications for pathogenesis, classification, and targeted therapies. *Cancer control : journal of the Moffitt Cancer Center* **16**, 8–13 (2009).

20 Thorne, L. G. *et al.* Evolution of enhanced innate immune evasion by SARS-CoV-2. *Nature* **602**, 487–495 (2022). https://doi.org/10.1038/s41586-021-04352-y

21 Loy, D. S. *et al.* SARS-CoV-2 surveillance and detection in wild, captive, and domesticated animals in Nebraska: 2021-2023. *Front Vet Sci* **11**, 1496207 (2024). https://doi.org/10.3389/fvets.2024.1496207

22 Lackey, J. A., Huckaby, D. G. & Ormiston, B. G. Peromyscus leucopus. *Mammalian Species*, 1–10 (1985). https://doi.org/10.2307/3503904

23 Ecke, F. *et al.* Population fluctuations and synanthropy explain transmission risk in rodent-borne zoonoses. *Nature communications* **13**, 7532 (2022). https://doi.org/10.1038/s41467-022-35273-7

24 Roy-Dufresne, E., Logan, T., Simon, J. A., Chmura, G. L. & Millien, V. Poleward expansion of the white-footed mouse (Peromyscus leucopus) under climate change: implications for the spread of lyme disease. *PloS one* **8**, e80724 (2013). https://doi.org/10.1371/journal.pone.0080724

25 Earnest, R. *et al.* Survey of white-footed mice (Peromyscus leucopus) in Connecticut, USA reveals low SARS-CoV-2 seroprevalence and infection with divergent betacoronaviruses. *npj Viruses* **1**, 10 (2023). https://doi.org/10.1038/s44298-023-00010-4

26 Ip, H. S. *et al.* An Opportunistic Survey Reveals an Unexpected Coronavirus Diversity Hotspot in North America. *Viruses* **13** (2021). https://doi.org/10.3390/v13102016

27 Phan, T. G. *et al.* The fecal viral flora of wild rodents. *PLoS pathogens* **7**, e1002218 (2011). https://doi.org/10.1371/journal.ppat.1002218

28 Gandhi, S. *et al.* De novo emergence of a remdesivir resistance mutation during treatment of persistent SARS-CoV-2 infection in an immunocompromised patient: A case report. *medRxiv* (2021). https://doi.org/10.1101/2021.11.08.21266069

29 Handrejk, K. *et al.* Characterization of a SARS-CoV-2 Omicron BA.5 direct-contact transmission model in hamsters. *Npj Viruses* **2**, 52 (2024). https://doi.org/10.1038/s44298-024-00061-1

30 Di Pietro, C. *et al.* Prior Influenza Infection Mitigates SARS-CoV-2 Disease in Syrian Hamsters. *Viruses* **16** (2024). https://doi.org/10.3390/v16020246

31 Wickenhagen, A. *et al.* Evolution of Omicron lineage towards increased fitness in the upper respiratory tract in the absence of severe lung pathology. *Nature communications* **16**, 594 (2025). https://doi.org/10.1038/s41467-025-55938-3

32 Uraki, R. *et al.* Characterization of SARS-CoV-2 Omicron BA.4 and BA.5 isolates in rodents. *Nature* **612**, 540–545 (2022). https://doi.org/10.1038/s41586-022-05482-7

33 Francis, M. E. *et al.* Previous infection with seasonal coronaviruses does not protect male Syrian hamsters from challenge with SARS-CoV-2. *Nature communications* **14**, 5990 (2023). https://doi.org/10.1038/s41467-023-41761-1

34 Tosta, E. The adaptation of SARS-CoV-2 to humans. *Mem Inst Oswaldo Cruz* **116**, e210127 (2022). https://doi.org/10.1590/0074-02760210127

35 Wise, A. G., Kiupel, M. & Maes, R. K. Molecular characterization of a novel coronavirus associated with epizootic catarrhal enteritis (ECE) in ferrets. *Virology* **349**, 164–174 (2006). https://doi.org/10.1016/j.virol.2006.01.031

36 Kenney, S. P., Wang, Q., Vlasova, A., Jung, K. & Saif, L. Naturally Occurring Animal Coronaviruses as Models for Studying Highly Pathogenic Human Coronaviral Disease. *Veterinary pathology* **58**, 438–452 (2021). https://doi.org/10.1177/0300985820980842

37 Gao, Y. Y. *et al.* An updated review of feline coronavirus: mind the two biotypes. *Virus Res* **326**, 199059 (2023). https://doi.org/10.1016/j.virusres.2023.199059

38 Buonavoglia, A., Pellegrini, F., Decaro, N., Galgano, M. & Pratelli, A. A One Health Perspective on Canine Coronavirus: A Wolf in Sheep's Clothing? *Microorganisms* **11** (2023). https://doi.org/10.3390/microorganisms11040921

39 He, H. *et al.* Transmission of HCoV-OC43 to pet hamsters. *Microb Pathog* **185**, 106364 (2023). https://doi.org/10.1016/j.micpath.2023.106364

40 Piggott, M. P. Effect of sample age and season of collection on the reliability of microsatellite genotyping of faecal DNA. *Wildlife Research* **31**, 485–493 (2004). https://doi.org/https://doi.org/10.1071/WR03096

41 Castañeda, D. *et al.* Absence of SARS-CoV-2 in wildlife of northeastern Minnesota and Isle Royale National Park. *Zoonoses Public Health* **71**, 744–747 (2024). https://doi.org/10.1111/zph.13162

42 Despres, H. W. *et al.* Surveillance of Vermont wildlife in 2021-2022 reveals no detected SARS-CoV-2 viral RNA. *Scientific reports* **13**, 14683 (2023). https://doi.org/10.1038/s41598-023-39232-0

43 Grace, S. G. *et al.* Low Prevalence of SARS-CoV-2 in Farmed and Free-Ranging White-Tailed Deer in Florida. *Viruses* **16** (2024). https://doi.org/10.3390/v16121886

44 Yao, W. *et al.* Evolution of SARS-CoV-2 Spikes shapes their binding affinities to animal ACE2 orthologs. *Microbiol Spectr* **11**, e0267623 (2023). https://doi.org/10.1128/spectrum.02676-23

45 Liu, Y. *et al.* Functional and genetic analysis of viral receptor ACE2 orthologs reveals a broad potential host range of SARS-CoV-2. *Proceedings of the National Academy of Sciences of the United States of America* **118** (2021). https://doi.org/10.1073/pnas.2025373118

46 Shi, K. *et al.* Structural basis of increased binding affinities of spikes from SARS-CoV-2 Omicron variants to rabbit and hare ACE2s reveals the expanding host tendency. *mBio* **15**, e0298823 (2024). https://doi.org/10.1128/mbio.02988-23

47 Park, E. S. *et al.* The comparison of pathogenicity among SARS-CoV-2 variants in domestic cats. *Scientific reports* **14**, 21815 (2024). https://doi.org/10.1038/s41598-024-71791-8

48 Lyoo, K. S. *et al.* Experimental Infection and Transmission of SARS-CoV-2 Delta and Omicron Variants among Beagle Dogs. *Emerg Infect Dis* **29**, 782–785 (2023). https://doi.org/10.3201/eid2904.221727

49 Kuhn, J. *et al.* Investigations on the Potential Role of Free-Ranging Wildlife as a Reservoir of SARS-CoV-2 in Switzerland. *Viruses* **16** (2024). https://doi.org/10.3390/v16091407

50 Vandegrift, K. J. *et al.* SARS-CoV-2 Omicron (B.1.1.529) Infection of Wild White-Tailed Deer in New York City. *Viruses* **14** (2022). https://doi.org/10.3390/v14122770

51 Bashor, L. *et al.* SARS-CoV-2 within-host population expansion, diversification and adaptation in zoo tigers, lions and hyenas. *bioRxiv* (2024). https://doi.org/10.1101/2024.10.24.620075

52 Tarbuck, N. N. *et al.* Persistence of SARS-CoV-2 Alpha Variant in White-Tailed Deer, Ohio, USA. *Emerg Infect Dis* **31**, 1319–1329 (2025). https://doi.org/10.3201/eid3107.241922

53 Yang, X. Y. *et al*. SARS-CoV-2 prevalence in wildlife 2020-2022: a worldwide systematic review and meta-analysis. *Microbes Infect* **26**, 105350 (2024). https://doi.org/10.1016/j.micinf.2024.105350

54 Ardalan, M. *et al.* Cattle, sheep, and goat humoral immune responses against SARS-CoV-2. *Vet Anim Sci* **26**, 100408 (2024). https://doi.org/10.1016/j.vas.2024.100408

55 Lee, L. K. F. *et al.* SARS-CoV-2 Surveillance of Wild Mice and Rats in North American Cities. *Ecohealth* **21**, 1–8 (2024). https://doi.org/10.1007/s10393-024-01679-6

56 Sims, M. *et al.* Suburban Population of Bobcats (Lynx rufus) in Connecticut, USA, Tested Negative for SARS-CoV-2, November 2021-February 2022. *Journal of wildlife diseases* **60**, 193–197 (2024). https://doi.org/10.7589/jwd-d-23-00054

57 Salajegheh Tazerji, S. *et al.* The risk of pet animals in spreading severe acute respiratory syndrome coronavirus 2 (SARS-CoV-2) and public health importance: An updated review. *Vet Med Sci* **10**, e1320 (2024). https://doi.org/10.1002/vms3.1320

58 Ferreira, F. C. *et al.* Respiratory Shedding of Infectious SARS-CoV-2 Omicron XBB.1.41.1 Lineage among Captive White-Tailed Deer, Texas, USA. *Emerg Infect Dis* **31**, 267–274 (2025). https://doi.org/10.3201/eid3102.241458

59 Kuchipudi, S. V. *et al.* Multiple spillovers from humans and onward transmission of SARS-CoV-2 in white-tailed deer. *Proceedings of the National Academy of Sciences of the United States of America* **119** (2022). https://doi.org/10.1073/pnas.2121644119

60 Beissat, K. *et al.* Infectious potential and circulation of SARS-CoV-2 in wild rats. *PloS one* **20**, e0316882 (2025). https://doi.org/10.1371/journal.pone.0316882

61 Wilson-Henjum, G. *et al.* Community-Scale Surveillance of SARS-CoV-2 and Influenza A Viruses in Wild Mammals, United States, 2022-2023. *Emerg Infect Dis* **31**, 1625–1629 (2025). https://doi.org/10.3201/eid3108.241671

62 Marchi, S. *et al.* Improving the ONE HEALTH approach: a lesson from SARS-CoV-2 pandemic. *J Prev Med Hyg* **65**, E312–E322 (2024). https://doi.org/10.15167/2421-4248/jpmh2024.65.3.3187

63 Vijgen, L. *et al.* Complete genomic sequence of human coronavirus OC43: molecular clock analysis suggests a relatively recent zoonotic coronavirus transmission event. *Journal of virology* **79**, 1595–1604 (2005). https://doi.org/10.1128/jvi.79.3.1595-1604.2005

64 Zhou, P. *et al.* Fatal swine acute diarrhoea syndrome caused by an HKU2-related coronavirus of bat origin. *Nature* **556**, 255–258 (2018). https://doi.org/10.1038/s41586-018-0010-9

65 Lednicky, J. A. *et al.* Independent infections of porcine deltacoronavirus among Haitian children. *Nature* **600**, 133–137 (2021). https://doi.org/10.1038/s41586-021-04111-z

66 Doyle, L. P. & Hutchings, L. M. A transmissible gastroenteritis in pigs. *Journal of the American Veterinary Medical Association* **108**, 257–259 (1946).

67 Attipa, C. *et al.* Emergence and spread of feline infection peritonitis due to a highly pathogenic canine/feline recombinant coronavirus. *bioRxiv*, 2023.2011.2008.566182 (2023). https://doi.org/10.1101/2023.11.08.566182

68 Percie du Sert, N. *et al.* The ARRIVE guidelines 2.0: Updated guidelines for reporting animal research. *PLoS biology* **18**, e3000410 (2020). https://doi.org/10.1371/journal.pbio.3000410

69 Sikes, R. S. 2016 Guidelines of the American Society of Mammalogists for the use of wild mammals in research and education. *J Mammal* **97**, 663–688 (2016). https://doi.org/10.1093/jmammal/gyw078

70 Bach, B. H. *et al.* Identifying individual ungulates from fecal DNA: a comparison of field collection methods to maximize efficiency, ease, and success. *Mammalian Biology* **102**, 863–874 (2022). https://doi.org/10.1007/s42991-021-00176-5

71 DeGraaf, R. M. & Rudis, D. D. New England wildlife: Habitat, natural history, and distribution. (U.S. Department of Agriculture, Forest Service, Northeastern Forest Experiment Station, 1986).

72 Xiu, L. *et al.* A RT-PCR assay for the detection of coronaviruses from four genera. *J Clin Virol* **128**, 104391 (2020). https://doi.org/10.1016/j.jcv.2020.104391

73 Thompson, J. D., Higgins, D. G. & Gibson, T. J. CLUSTAL W: improving the sensitivity of progressive multiple sequence alignment through sequence weighting, position-specific gap penalties and weight matrix choice. *Nucleic acids research* **22**, 4673–4680 (1994). https://doi.org/10.1093/nar/22.22.4673

74 Tamura, K., Stecher, G. & Kumar, S. MEGA11: Molecular Evolutionary Genetics Analysis Version 11. *Mol Biol Evol* **38**, 3022–3027 (2021). https://doi.org/10.1093/molbev/msab120

75 Matranga, C. B. *et al.* Enhanced methods for unbiased deep sequencing of Lassa and Ebola RNA viruses from clinical and biological samples. *Genome biology* **15**, 519 (2014). https://doi.org/10.1186/preaccept-1698056557139770

76 Kalantar, K. L. *et al.* IDseq-An open source cloud-based pipeline and analysis service for metagenomic pathogen detection and monitoring. *Gigascience* **9** (2020). https://doi.org/10.1093/gigascience/giaa111

77 Ramesh, A. *et al.* Metagenomic next-generation sequencing of samples from pediatric febrile illness in Tororo, Uganda. *PloS one* **14**, e0218318 (2019). https://doi.org/10.1371/journal.pone.0218318

78 Courtney, P. A. & Fenton, M. B. The Effects of a Small Rural Garbage Dump on Populations of Peromyscus leucopus Rafinesque and Other Small Mammals. *Journal of Applied Ecology* **13**, 413–422 (1976). https://doi.org/10.2307/2401790

79 Zeiss, C. J., Asher, J. L., Vander Wyk, B., Allore, H. G. & Compton, S. R. Modeling SARS-CoV-2 propagation using rat coronavirus-associated shedding and transmission. *PloS one* **16**, e0260038 (2021). https://doi.org/10.1371/journal.pone.0260038

80 Thi Nhu Thao, T. *et al.* Rapid reconstruction of SARS-CoV-2 using a synthetic genomics platform. *Nature* **582**, 561–565 (2020). https://doi.org/10.1038/s41586-020-2294-9

81 Lindenbach, B. D. & Rice, C. M. trans-Complementation of yellow fever virus NS1 reveals a role in early RNA replication. *Journal of virology* **71**, 9608–9617 (1997). https://doi.org/10.1128/jvi.71.12.9608-9617.1997

82 Matsuyama, S. *et al.* Enhanced isolation of SARS-CoV-2 by TMPRSS2-expressing cells. *Proceedings of the National Academy of Sciences* **117**, 7001–7003 (2020). https://doi.org/doi:10.1073/pnas.2002589117

83 Gruber, A. D. *et al.* Standardization of Reporting Criteria for Lung Pathology in SARS-CoV-2-infected Hamsters: What Matters? *American journal of respiratory cell and molecular biology* **63**, 856–859 (2020). https://doi.org/10.1165/rcmb.2020-0280LE

84 Schmittgen, T. D. & Livak, K. J. Analyzing real-time PCR data by the comparative C(T) method. *Nature protocols* **3**, 1101–1108 (2008). https://doi.org/10.1038/nprot.2008.73

Author contributions:

SI: Design, acquisition, analysis, interpretation of data, initial draft

SC: Design, acquisition, analysis, interpretation of data, initial draft

MB: Acquisition of data, initial draft

SR: Acquisition of data

NG: Design, analysis, interpretation of data, initial draft

WT: Acquisition of data

M: Acquisition of data, initial draft

SW: Acquisition of data, initial draft

KZ: Design, acquisition of data

GWC: Design, acquisition of data

JL: Design, acquisition of data

MS: Acquisition of data

GR: Design, conceptualization, acquisition of data

WT: Acquisition of data

CZ: Design, conceptualization, acquisition and interpretation of data, initial draft

Figure legends

Figure 1: Locations of surveyed mammals, excluding *P. leucopus* (n=407).
Pan CoV-negative cases are indicated with a small black circle. Pan CoV-positive cases are color coded by identity of CoV on BLAST sequence analysis (see Table 1). All instances represent a single animal, except for bovine cases mapping to the same farm (n=8). Mapped using ARC GIS (https://www.arcgis.com/), underlaid with population density. The majority of samples were derived from Connecticut, with fewer samples from New York, Rhode island and Massachusetts.

Figure 2: Locations of surveyed *P. leucopus* (n= 482). Pan-CoV negative cases are indicated with a small black circle. Pan-CoV positive cases indicated in red (n=19) in insets. Mapped using ARC GIS, numbers clustered by location in overview map, unclustered in insets. All samples were derived from Connecticut.

Figure 3: Multiple sequence alignment utilizing Pan-CoV PCR derived RdRp sequences. Samples are outlined by color shown in the accompanying species icons. These are: WFM (blue), bovine (purple), cat

(green), dog (orange), sheep (grey), goat (gold), red panda (red), ferret (light green), woodchuck (light blue). WFM mouse sequences cluster with the recently described *Peromyscus betacoronavirus* [25] . Reference sequences are uncolored. Multiple sequence alignments and phylogenetic tree were prepared using the Clustal W and MEGA11 programs with default parameters and the neighbour-joining method with 1000 bootstrap replicates.

Figure 4. Viral RNA shedding (cycle number) following SARS-CoV-2 ancestral and Omicron BA5 infection in white-footed mice and Syrian hamsters via different routes.

a, b: Naïve WFM (a) and Syrian hamsters (b) were infected intranasally with 10^5PFU of SARS-CoV-2 ancestral or Omicron BA5 strains respectively. Oronasal viral RNA shedding in these animals is shown.

c: Naive WFM infected with ancestral or Omicron BA5 strains were cohoused with naïve animals for two days (indicated with blue boxes). Oronasal viral RNA shedding in naïve contact animals is shown.

d: Naive Syrian hamsters were housed in cages vacated by infected WFM (those shown in A) for 7 days. Oronasal viral RNA shedding in these hamsters is shown. Oral swab viral RNA shedding expressed in cycle numbers visualized using a heatmap (lower Cq=red, higher Cq=green). Days post infection shown above, with cohousing days shown in blue. A total of 24 WFM, evenly split by sex, were used for inoculation and transmission experiments. Six hamsters were used in each fomite exposure group (total n=12). An additional 12 mock-inoculated (DMEM) WFM (n=6) and hamsters (n=6) were used as a negative control group. All groups were evenly split by sex. Red hatches indicate euthanasia of animals (n=3) due to causes unrelated to experimental procedures (fight wounds).